Journal of Magnetic Resonance 199 (2009) 208–213

Contents lists available at ScienceDirect

Journal of Magnetic Resonance

journal homepage: www.elsevier.com/locate/jmr

Why does PMLG proton decoupling work at 65 kHz MAS?

Michal Leskes [a], P.K. Madhu [b,*], Shimon Vega [a]

[a] Department of Chemical Physics, Weizmann Institute of Science, Rehovot 76100, Israel
[b] Department of Chemical Sciences, Tata Institute of Fundamental Research, Homi Bhabha Road, Colaba, Mumbai 400 005, India

ARTICLE INFO

Article history:
Received 24 February 2009
Revised 3 May 2009
Available online 12 May 2009

Keywords:
Solid-state NMR
Homonuclear dipolar decoupling
PMLG
Fast MAS
Floquet theory

ABSTRACT

Schemes such as phase-modulated Lee–Goldburg (PMLG) for homonuclear dipolar decoupling have been shown to yield high-resolution ^{1}H spectra at high magic-angle spinning (MAS) frequencies of 50–70 kHz. This is at variance to the commonly held notion that these methods require MAS frequencies not comparable to the cycle frequencies of the pulse schemes. Here, a theoretical argument, based on bimodal Floquet theory, is presented to explain this aspect together with conditions where PMLG type of schemes may be successful at high MAS frequencies.

1. Introduction

High-resolution ^{1}H NMR spectra of solids are best obtained with a combination of magic-angle spinning (MAS) and homonuclear dipolar decoupling radiofrequency (RF) pulse schemes. A variety of pulse schemes has been designed for this purpose [1–3]. The initial schemes introduced for static samples were also found suitable for application at what is considered today low spinning frequencies. Sequences such as MREV8, BR24, BLEW12, TREV8, CORY24, and MSHOT3 [4–14] are efficient when applied at the quasi static limit when the RF cycle time, τ_c, is much shorter than the sample spinning period, τ_r. The two averaging processes can then be considered separately, ignoring interference between them.

As higher MAS frequencies became possible, newer sequences were required for homonuclear dipolar decoupling, prominent among them being the PMLG scheme [15,16], which originated from the FSLG scheme [17,18], and the DUMBO method [19]. These two techniques have been used in the characterisation of various organic and inorganic compounds [20]. Insertion of detection windows between the repeating units of pulses allowed the acquisition of high-resolution one-dimensional ^{1}H spectra [21,22]. Both the techniques are applied non-synchronous with the rotor period, a condition which is crucial for avoiding recoupling of the dipolar interaction. This condition requires that $n\tau_c \neq k\tau_r$, with n and k integers and $1 \leqslant |n| \leqslant 4$. To avoid recoupling at MAS frequencies up to 25 kHz, the RF cycle time was chosen as short as possible. Specifically, this then required that $3\tau_c < \tau_r$ and $4\tau_c \neq \tau_r$, as was shown experimentally for both PMLG [16] and DUMBO [22]. This requirement would lead to pulse durations of the order of 1–2 μs for a typical experiment with *w*PMLG5 at RF amplitudes of the order of 80–140 kHz.

In the last couple of years ultra-fast MAS probes have become available making spinning frequencies up to 70 kHz possible [23]. Combining such spinning frequencies with the PMLG scheme and maintaining $\tau_r/\tau_c \approx 3.5$ to avoid line-broadening resonances, extremely short pulses (less than 200 ns for *w*PMLG5 at 60 kHz MAS) would be required leading to unrealistic RF amplitudes. Therefore, it was expected that other conditions are needed for applying PMLG type decoupling at these high spinning frequencies.

Lately two other homonuclear dipolar decoupling experiments have been suggested which are based on the symmetry principles and applied synchronised with MAS: the *R*-symmetry based sequence composed of composite π pulses [24,25] and the smooth amplitude modulation [26,27]. These schemes were applied at MAS frequencies up to 30 kHz [25] and 65 kHz [26], respectively. The potential application of the *R*-based sequence at MAS frequencies of the order of 60 kHz with moderate RF amplitudes was shown numerically [25].

Recently, we have shown that contrary to the expectations based on our experience at moderate MAS frequencies, supercycled *w*PMLG and *w*DUMBO can be applied successfully at 65 kHz spinning speed [28]. It was surprising to observe that high resolution can be achieved with RF cycle times comparable and longer than that of the rotor period such that $\tau_r/\tau_c < 1$. The short *w*PMLG5 cycle

* Corresponding author. Fax: +91 22 2280 4610.
E-mail addresses: madhu@tifr.res.in (P.K. Madhu), shimon.vega@weizmann.ac.il (S. Vega).

1090-7807/$ - see front matter © 2009 Elsevier Inc. All rights reserved.
doi:10.1016/j.jmr.2009.05.003

times (with pulse durations of the order of 700 ns and detection windows of 3.2 μs), accompanied by a high RF amplitude (up to 250 kHz), lead to comparable and in some cases slightly better resolution than that obtained at lower MAS frequencies. Another demonstration of the combination of DUMBO with very fast MAS was provided very recently focusing on the high sensitivity gained at such MAS frequencies [29].

Here we will provide a theoretical explanation for the high resolution achieved under conditions of comparable RF and MAS cycle times. We will show that at high MAS frequencies the effect of the line broadening resonances becomes very narrow and localised, thus allowing the cycle time to be set very close to their exact position. The effect of degeneracies due to synchronisation between the MAS and RF periodicities will be reviewed and line broadening factors will be derived based on bimodal Floquet theory [30,31]. The extent of the deleterious effect of such degeneracies will be demonstrated by calculations for the supercycled PMLG5 scheme and compared with numerical simulations.

2. Theory

A system of coupled protons subjected to MAS and to an RF decoupling sequence can be described by the following bimodal Floquet Hamiltonian in the RF interaction frame:

$$H_F = \sum_{n,k}(H^{CS}_{nk} + H^{D}_{nk}) + \omega_r N^r + \omega_c N^c \tag{1}$$

$$H^{cs}_{nk} = \sum_{a,m} \Delta\omega_a d^{(1)}_{m,k} T^{(1)}_{m,a} F^r_0 F^c_k \tag{2}$$

$$H^{D}_{nk} = \sum_{a<b,m} \omega_{ab} G^{ab}_n d^{(2)}_{m,k} T^{(2)}_{m,ab} F^r_n F^c_k \tag{3}$$

where $\omega_r = 2\pi/\tau_r$ and $\omega_c = 2\pi/\tau_c$ are the characteristic frequencies of MAS and RF sequence, respectively. The interactions considered here are the isotropic chemical shift (CS) of spin a with magnitude $\Delta\omega_a$ and the homonuclear dipolar interactions with coupling frequencies ω_{ab}. The $d^{(l)}_{m,k}$ coefficients are the Fourier coefficients describing the time dependence of the chemical shifts ($l = 1$) and dipolar interactions ($l = 2$) in the RF interaction frame. They depend on the sequence of pulses used for decoupling. The G^{ab}_n coefficients describe the geometrical dependence of the time dependent anisotropic dipolar interaction due to MAS which are non-zero for $n = \pm1$, ±2 [32]. The $T^{(l)}_m$'s are the irreducible tensor spin operators. The N and F operators are the number and ladder operators, respectively [33].

In order to evaluate the effect of MAS frequencies on the dipolar interaction, we can derive an effective Hamiltonian using the van Vleck transformation [34]. This transformation is defined only when there are no zero-order degeneracies in the Floquet Hamiltonian. Such degeneracies occur when the two periodicities are chosen such that $n\omega_r + k\omega_c = 0$. For these values diagonal block elements $\omega_r N^r + \omega_c N^c$ in the Floquet Hamiltonian become equal. If the degenerate diagonal block elements are connected by off-diagonal elements of the form $\langle n'k'|H_{nk}|n''k''\rangle \neq 0$ with $n = n' - n''$ and $k = k' - k''$ the van Vleck transformation cannot be applied and these off-diagonal elements significantly contribute to the effective Hamiltonian. Since the dipolar part of the Hamiltonian has off-diagonal elements with $|n| = 1,2$ and $k \neq 0$, these zero order degeneracies can cause severe dipolar line broadening.

For characteristic frequencies, which do not lead to a zero-order degeneracy, we can apply a van Vleck transformation and truncate the small and non-significant terms obtained after the transformation. Leaving only the zero- and first-order terms leads to the following Hamiltonian

$$\tilde{H}_F = \tilde{H}^{CS(0)}_{00} + \sum_{n,k}\left(\tilde{H}^{CS(1)}_{0k} + \tilde{H}^{D(1)}_{nk}\right) + \omega_r N^r + \omega_c N^c \tag{4}$$

$$\tilde{H}^{CS(0)}_{00} = \sum_{a,m} \Delta\omega_a d^{(1)}_{m,0} T^{(1)}_{m,a} F^r_0 F^c_0 \tag{5}$$

$$\tilde{H}^{CS(1)}_{0k} = -\frac{1}{2}\sum_{k' \neq 0,a,m,m'} \Delta\omega_a^2 \frac{d^{(1)}_{m,k'} d^{(1)}_{m',k-k'}}{k'\omega_c}\left[T^{(1)}_{m,a}, T^{(1)}_{m',a}\right] F^r_0 F^c_k \tag{6}$$

$$\tilde{H}^{D(1)}_{nk} = -\frac{1}{2}\sum_{m,m',n',a<b,b<c} \omega_{ab}\omega_{bc} G^{ab}_{n'} G^{bc}_{n-n'} \Delta^{n',k}_{m,m'}\left[T^{(2)}_{m,ab}, T^{(2)}_{m',bc}\right] F^r_n F^c_k \tag{7}$$

with

$$\Delta^{n',k}_{m,m'} = \sum_{k'} \frac{d^{(2)}_{m,k'} d^{(2)}_{m',k-k'}}{\omega_r(n' + k'\psi)} \tag{8}$$

and $\psi = \omega_c/\omega_r$. $\tilde{H}^{CS(0)}_{00}$ and $\tilde{H}^{CS(1)}_{0k}$ are the zero-order (diagonal) and first-order (diagonal and off diagonal) contributions to the chemical-shift interaction, respectively. The zero-order term defines the scale factor of the chemical shift which is given by

$$s = \sqrt{\sum_m \left|d^{(1)}_{m,0}\right|^2} \tag{9}$$

$\tilde{H}^{D(1)}_{nk}$ is the first-order (diagonal and off-diagonal) dipolar Hamiltonian which should be reduced as best as possible by the RF decoupling scheme for spectral line narrowing.

It is convenient to define the diagonal blocks of this Hamiltonian as

$$\bar{H}_F = \left(\tilde{H}^{CS(0)}_{00} + \tilde{H}^{CS(1)}_{00} + \tilde{H}^{D(1)}_{00}\right) + \omega_r N^r + \omega_c N^c \tag{10}$$

which can be derived by substituting $n = k = 0$ in Eq. (4). The diagonal elements form the effective Hamiltonian $H_{\text{eff}} = \langle 00 \mid \tilde{H}^{CS(0)}_{00} + \tilde{H}^{CS(1)}_{00} + \tilde{H}^{D(1)}_{00} \mid 00\rangle$. This effective Hamiltonian can be used to evaluate the efficiency of the decoupling sequence as long as we can ignore the off-diagonal block elements. The dipolar interaction is reduced under the influence of the RF pulses and MAS when the $\Delta^{n',0}_{m,m'}-$ terms in Eq. (8) are minimised. However, when $n\omega_r + k\omega_c = 0$, the off-diagonal blocks of the form $\langle n'k' \mid \tilde{H}^{D(1)}_{nk} \mid n''k''\rangle \neq 0$, with $|n| = |n' - n''| = 1,2,3,4$ and $|k| = |k' - k''| \neq 0$, become important. Thus we have two types of degeneracy conditions leading to line broadening: zero order, which are formed in the original Floquet Hamiltonian, and first order which are expected to have a less pronounced effect on the spectrum since their off-diagonal blocks are smaller. The possible zero-order and first-order recoupling conditions for different ratios of $\psi = \omega_c/\omega_r$ with $n = 1,2$ and $n = 3,4$ and $-15 \leqslant k \leqslant -1$ are plotted in Fig. 1. Each line in this plot corresponds to one of the conditions with $\psi = |n/k|$. Only degeneracies connected by non-zero off-diagonal blocks will lead to deterioration in decoupling. The conditions are very dense in the region of $\psi \leqslant 1.5$ and are relatively sparse above that. Beyond $\psi = 2$ only two isolated first-order conditions are formed. This dense set of degeneracies for $\psi \leqslant 1.5$ lead to the assumption that PMLG based decoupling sequences are more suitable for application at moderate MAS frequencies, where ψ ratios larger than three are experimentally feasible [21]. The fact that degeneracies in the Hamiltonian have a deleterious effect over a certain width supports further the practice of avoiding the application of decoupling schemes with MAS frequencies close to the degeneracy condition.

To achieve spectral line narrowing the pulse sequences should lead to both the minimisation of the dipolar Δ-coefficients defined in Eq. (8) and the maximisation of the scaled chemical shift, given by Eq. (9). Away from the degeneracy conditions it suffices to consider the diagonal contributions of the $\Delta^{n',0}_{m,m'}$-coefficients. Combining these two requirements we can define a parameter which is related to the efficiency of decoupling:

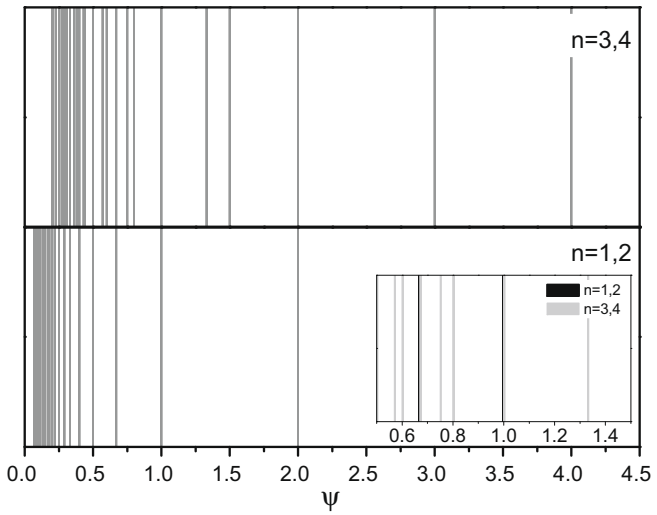

Fig. 1. The positions of the possible zero- and first-order degeneracies (given by n/k) as a function of $\psi = \omega_c/\omega_r$. The $\{n = 3,4; 1 \leqslant k \leqslant 15\}$ and the $\{n = 1,2; 1 \leqslant k \leqslant 15\}$ conditions are plotted in the top and bottom row, respectively. The former can be connected by a first-order off-diagonal element and the later by both zero- and first-order ones. In the inset the region of $0.5 \leqslant \psi \leqslant 1.5$ is plotted with black lines corresponding to zero-order and the gray lines to first-order conditions.

$$\chi^2 = \frac{\sum_{n',m \geqslant m'} |\Delta^{n',0}_{m,m'}|^2}{\sum_{m''} |d^{(1)}_{m'',0}|^2} \tag{11}$$

χ is dependent on the Fourier coefficients of the decoupling sequence and therefore it will change according to the values of the experimental parameters, such as the RF amplitude ω_1 and the pulse duration τ_p. It is also sensitive to changes in ψ, through the denominator of the Δ-coefficients. An increase in the value of the Δ-coefficients is expected when ψ approaches the condition $n + k\psi = 0$. Obviously, close to and at these degeneracy conditions χ cannot be used to evaluate decoupling.

We can estimate the region where χ is not valid by putting limits on the magnitude of the off-diagonal block coefficients:

$$3 \times \left|\langle n'k'|H|n''k''\rangle\right| > \left|(n' - n'')\omega_r + (k' - k'')\omega_c\right| \tag{12}$$

Here $H = H_F$ for zero-order and $H = \tilde{H}_F$ for first-order degeneracies. In the first case, the connecting off-diagonal terms are proportional to $\omega_{ab} G^{ab}_n d^{(2)}_{m,k}$ with all the m values possible. In the second case, the connecting terms are proportional to the Δ-coefficients in Eq. (8) with $n,k \neq 0$.

We will now focus on the supercycled PMLG5 [35,36] pulse sequence and concentrate on the region $0.5 < \psi < 1.5$ where the zero- and first-order degeneracy conditions are dense, as plotted in the inset of Fig. 1. This region corresponds to ω_c values that are feasible experimentally for fast MAS. The effect of MAS and RF frequencies on the width of the degeneracy conditions will be examined.

3. Results and discussion

The efficiency of decoupling upon combining MAS and PMLG5$^{\bar{x}x}_{mm}$ defined by the parameter χ is plotted in Fig. 2. The contours are result of calculations performed for four values of $\nu_c = \omega_c/2\pi$: 20 kHz with $\tau_c = 50$ μs and $\tau_p = 2.5$ μs, 30 kHz with $\tau_c = 33.33$ μs and $\tau_p = 1.67$ μs, 40 kHz with $\tau_c = 25$ μs and $\tau_p = 1.25$ μs, and 50 kHz with $\tau_c = 20$ μs and $\tau_p = 1$ μs. For each ν_c value, χ was calculated as a function of the RF amplitude ($\nu_1 = 60$–280 kHz, showing only the relevant regions) and ψ by varying the MAS frequency $\nu_r = \omega_r/2\pi$. The ratio of the characteristic frequencies was chosen between $0.5 < \psi \leqslant 2.2$, with $\psi \neq 1,2$. This corresponds to spinning frequencies ν_r in the range of 10–100 kHz. The χ values were multiplied by 100 kHz^2 to present the magnitude of the dipolar frequencies and the geometrical coefficients. As a result the values plotted in the contours vary between 0 and 6 kHz. The lines added to the contours indicate the regions where χ is not a valid parameter for evaluating the decoupling effi-

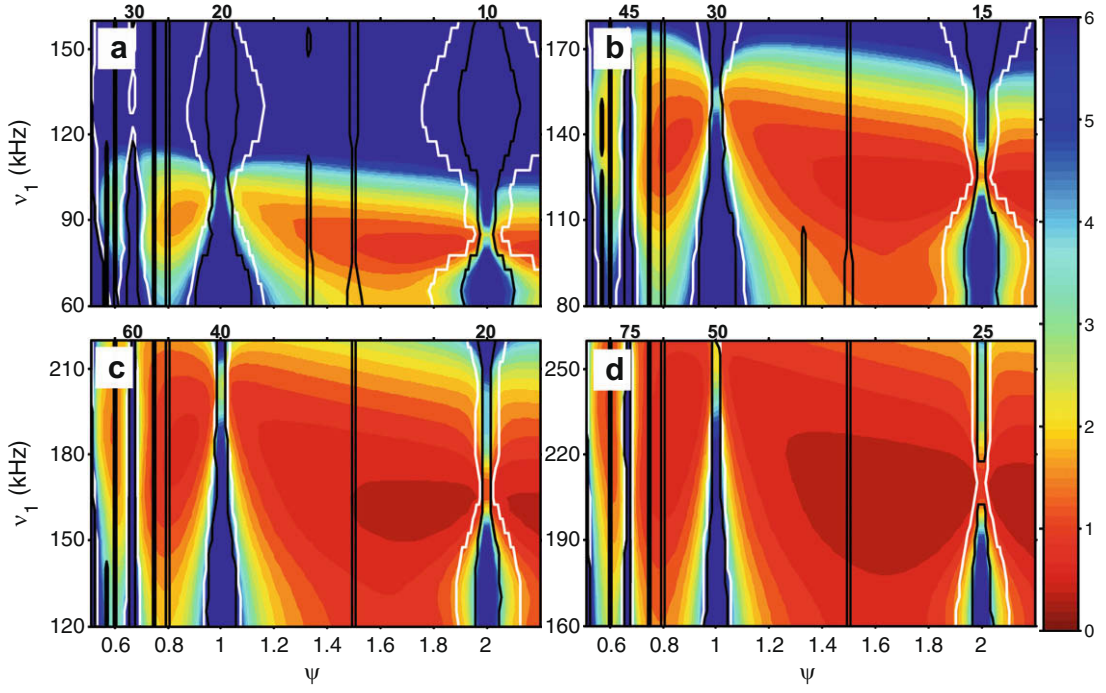

Fig. 2. The magnitude of the χ parameter multiplied by 100 kHz^2 as a function of the RF amplitude ν_1 and ψ for the PMLG5$^{\bar{x}x}_{mm}$ sequence with cycle frequencies of (a) 20, (b) 30, (c) 40, and (d) 50 kHz. The white lines specify regions where the zero-order off-diagonal elements become significant and the χ parameter cannot be used to evaluate the extent of decoupling. The first-order regions are plotted in black. The numbers in bold on the top of each figure are the MAS frequencies in kHz.

ciency. In these regions the off-diagonal blocks become significant and their values pass the threshold defined in Eq. (12). For these calculations we have used all values $|n| = 1,2$ and $|k| \leqslant 100$ for the zero-order off-diagonal elements (plotted in white) and $|n| = 1-4$ and $|k| \leqslant 50$ for the first-order ones (plotted in black). In both cases the threshold was checked for all combinations of n, k, and m.

The parameter χ itself is sensitive only to the zero-order degeneracy conditions, when the denominator of the Δ-coefficients becomes zero. The width of the region where the zero-order degeneracies influence the decoupling can thus also be obtained from the magnitude of χ. These zero-order degeneracy bands are clearly observed in Fig. 2 for $\psi = 1/2, 2/3, 1, 2$. The width of these regions increases for increasing ψ. The width of the first-order degeneracy regions cannot be directly obtained by evaluating χ. They are indicated by the black line bordered regions. Their width is relatively narrow, as expected.

In Fig. 2, from a to d, the parameters defining the PMLG5$^{\bar{x}x}_{mm}$ decoupling experiment, ν_c, ν_r, and ν_1, are all increased. Thus, it is not surprising that overall there is an improvement in decoupling and a decrease in χ. These three experimental parameters have practical limitations, which lead to the fact that fast MAS at 40–65 kHz cannot be applied with 50 kHz < ν_c (for the super cycled PMLG5 scheme with 20 pulses per cycle, placing limitation on pulse lengths to be longer than 1 μs and RF amplitude to be lower than 250 kHz). The limit on the ratio for this MAS range is therefore $\psi \leqslant 1.25$ and, as shown Fig. 1, in this region degeneracies are very abundant. For low MAS frequencies higher ψ values can be reached and are preferred for staying away from the degeneracy bands. The width of these degeneracy bands is important when we are forced to operate in their vicinities and this becomes crucial at high MAS frequencies. Ignoring the overall increase in χ with longer PMLG pulse sequences, the width of the degeneracy bands decreases for increasing ν_c, as is clearly observed around $\psi = 1$ going from $\nu_c = 20$ kHz (top left) to 50 kHz (bottom right). The narrowing of the local effect of the degeneracy conditions in the range $\psi \leqslant 1.25$ required for the fast MAS experiments allows us to acquire high-resolution spectra at these spinning frequencies. However, resolution expected in this regime is comparable to that at moderate MAS frequencies operating at much higher values of ψ.

In order to verify the validity of χ as a parameter to determining the extent of decoupling, we performed numerical simulations using the SPINEVOLUTION program [37]. These simulations were performed for a system of three protons with coordinates representing a $(C)H^a-(C)H_2^{b,c}$ molecular fragment. The dipolar interaction strengths for this system are 7.7, 4.2, and 23 kHz for the spin pairs *ab*, *ac*, and *bc*, respectively. Spectra were calculated using the PMLG5$^{\bar{x}x}_{mm}$ sequence with $\nu_c = 20$–50 kHz as a function of ψ by varying the MAS frequency. The RF amplitude was chosen according to the Lee–Goldburg (LG) condition $\nu_1 = \sqrt{2/3}/(5\tau_p)$, where τ_p is the length of a single PMLG pulse. As discussed in Ref. [38] the LG condition does not necessarily correspond to the optimum RF amplitude for decoupling (combining PMLG pulses with MAS it was shown that the deviations from the LG condition are significant in particular when ω_c and ω_r are increased). In Fig. 3a, the full width at half height of the simulated proton-*a* line is plotted for four cycle frequencies (the values of the RF amplitudes are specified at the inset). In Fig. 3b, we have plotted the parameter χ calculated with the values used in our simulations. The result corresponds to horizontal cuts through the contour plots in Fig. 2 at the specified ν_1 values. The open and filled circles were calculated for moderate MAS frequencies. Their sensitivity to the degeneracy conditions is relatively high, as reflected by the fwhh values close to $\psi = 1/2, 2/3, 1, 2$. An additional small broadening is observed at $\psi = 3/2$, as expected from the first-order degeneracy condition. In the fast MAS range simulations (half-filled circles) the effect of the degeneracies on the fwhh is confined to about

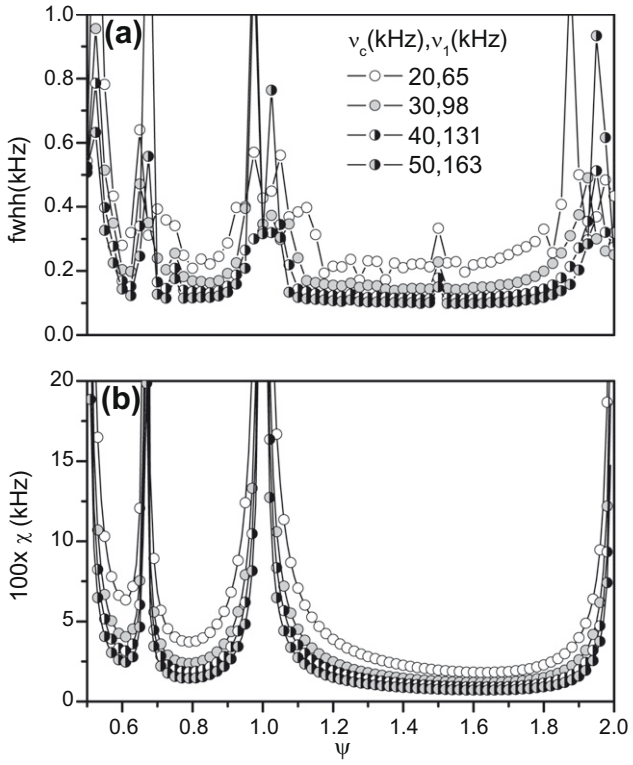

Fig. 3. (a) The full width at half height of the spectral line of proton *a* in a H^a–$H^{b,c}$ spin system simulated with SPINEVOLUTION for PMLG5$^{\bar{x}x}_{mm}$ sequence applied with varying RF periodicity and amplitudes as specified in the figure. (b) Cuts in the contour plots in Fig. 2 of the χ parameter taken at the corresponding ν_1 values used for the simulation.

$\psi \pm 0.1$. The χ parameter (Fig. 3b) shows the same general trend as the fwhh obtained from simulations (Fig. 3a).

Finally, in order to show that the resolution achieved by combining fast MAS with PMLG5$^{\bar{x}x}_{mm}$ at $\psi < 1$ is comparable to that obtained with moderate MAS frequencies and higher ψ values, we have performed a simulation on a five spins system (coordinates and chemical shift as in Ref. [39]). The result is shown in Fig. 4 for $\nu_c \approx 50$ kHz. The middle spectrum was simulated for $\nu_r = 20$ kHz and $\psi = 2.5$ and the best resolution was achieved with $\nu_1 = 130$ kHz. For the top spectrum with $\nu_r = 65$ kHz and $\psi = 0.775$ the best resolution was achieved for $\nu_1 = 250$ kHz. These simulations can be correlated to the χ parameters by their values plotted on the right of each spectrum where only the relevant region of the calculation is shown. The black point marks the parameters approximately corresponding to those used in the simulations. The two spectra have similar resolution despite the fact that the fast MAS simulation is done for a ψ value between the two first-order degeneracies ($\psi = 3/4, 4/5$) and close to a zero-order one ($\psi = 2/3$). The necessary increase in the RF amplitude agrees with the calculation of the χ parameter in Fig. 2. The same resolution cannot be achieved at 20 kHz MAS with $\psi = 0.775$, as shown in the bottom spectrum calculated with $\nu_1 = 75$ kHz. Although the corresponding χ parameter plotted on the right was calculated for $\nu_c = 20$ kHz (and not 16 kHz as in the simulation) it does reflect the lower resolution achieved and the width of the degeneracy conditions at this low MAS frequency.

4. Conclusions

We have shown that the acquisition of high-resolution proton spectra by a combination of PMLG and fast MAS with compara-

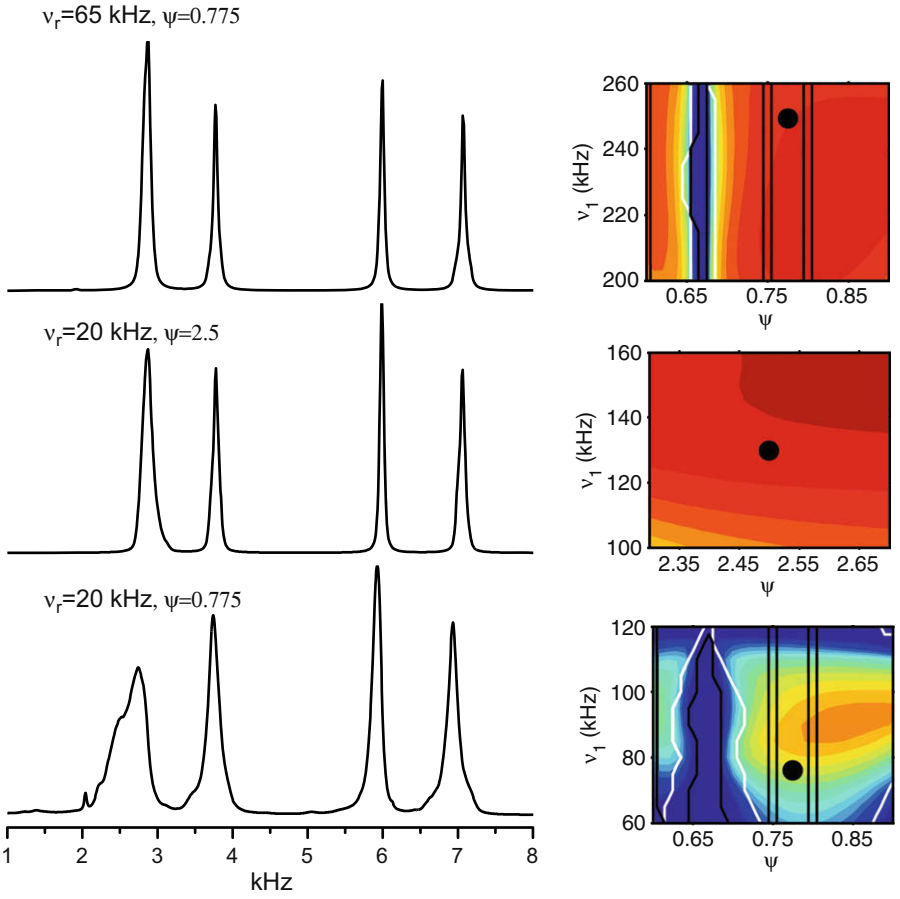

Fig. 4. Simulated ^{1}H spectra of a five spins system with PMLG5$^{\bar{x}x}_{mm}$ and MAS frequency of 65 kHz (top) and 20 kHz (middle and bottom). The pulse length and the RF amplitude used were 1 μs and 250 kHz for the top spectrum, 1 μs and 130 kHz for the middle spectrum, and 3.2 μs and 75 kHz for the bottom spectrum. On the right side of each spectrum the relevant region from the contour plots in Fig. 2 is shown. For the top and middle rows ν_c was 50 kHz at which χ shown was calculated. For the bottom row ν_c = 15.6 kHz and χ was calculated for ν_c = 20 kHz. The black point corresponds to the parameters used for the simulation and the colour coding is the same as in Fig. 2.

ble RF and MAS cycle times is possible due to the relatively narrow regimes around the degeneracy conditions defined by the ratio between the characteristic frequencies. These conditions are much broader at lower MAS frequencies and must be avoided by setting the RF cycle time much shorter than the rotor period. As there is no improvement in resolution when increasing the MAS frequency and RF amplitudes, from the point of view of proton resolution, intermediate MAS frequencies are still preferable. However, when we are interested in correlating protons with nuclei possessing large chemical-shift anisotropies, fast MAS frequencies are very beneficial without loosing proton resolution.

Acknowledgment

We acknowledge support from the Israel Science Foundation. The research is made possible in part by the historic generosity of the Harold Perlman family.

References

[1] C.E. Bronnimann, B.L. Hawkins, M. Zhang, G.E. Maciel, Combined rotation and multiple pulse spectrosocpy as an analytical proton nuclear magnetic resonance technique for solids, Anal. Chem. 60 (1988) 1743–1750.
[2] B.C. Gerstein, C. Clor, R.G. Pembelton, R.C. Wilson, Utility of pulse nuclear magnetic resonance in studying protons in coals, J. Phys. Chem. 81 (1977) 565.
[3] E. Vinogradov, P.K. Madhu, S. Vega, Strategies for high-resolution proton spectroscopy in solid-state NMR, Topics Curr. Chem. 246 (2005) 33.
[4] P. Mansfield, Symmetrized pulse sequences in high resolution NMR in solids, J. Phys. C Solid State Phys. 4 (1971) 1444.
[5] W.-K. Rhim, A. Pines, J.S. Waugh, Time-reversal experiments in dipolar-coupled spin systems, Phys. Rev. B3 (1971) 684–696.
[6] M. Mehring, J.S. Waugh, Magic-angle NMR experiments in solids, Phys. Rev. B5 (1972) 3459.
[7] W.-K. Rhim, E.E. Elleman, R.W. Vaughan, Analysis of multiple pulse NMR in solids, J. Chem. Phys. 59 (1973) 3740–3749.
[8] D.P. Burum, W.-K. Rhim, Analysis of multiple pulse NMR in solids-part 3, J. Chem. Phys. 71 (1979) 944–956.
[9] D.P. Burum, W.-K. Rhim, An improved NMR technique for homonuclear dipolar decoupling in solids: application to polycrystalline ice, J. Chem. Phys. 70 (1979) 3553–3554.
[10] D.P. Burum, M. Linder, R.R. Ernst, Low-power multipulse line narrowing in solid-state NMR, J. Magn. Reson. 44 (1981) 173–188.
[11] K. Takegoshi, C.A. McDowell, A "magic echo" pulse sequence for the high-resolution NMR spectra of abundant spins in solids, Chem. Phys. Lett. 116 (1985) 100–104.
[12] D.G. Cory, A new multiple-pulse cycle for homonuclear dipolar decoupling, J. Magn. Reson. 94 (1991) 526–534.
[13] M. Hohwy, N.C. Nielsen, Elimination of high order terms in multiple pulse nuclear magnetic resonance spectroscopy: application to homonuclear decoupling in solids, J. Chem. Phys. 106 (1997) 7571–7586.
[14] M. Hohwy, P.V. Bower, H.J. Jakobsen, N.C. Nielsen, A high-order and broadband CRAMPS experiment using z-rotational decoupling, Chem. Phys. Lett. 273 (1997) 297–303.
[15] E. Vinogradov, P.K. Madhu, S. Vega, High-resolution proton solid-state NMR spectroscopy by phase-modulated Lee–Goldburg experiment, Chem. Phys. Lett. 314 (1999) 443–450.
[16] E. Vinogradov, P.K. Madhu, S. Vega, Phase modulated Lee–Goldburg magic angle spinning proton nuclear magnetic resonance experiments in the solid state: a bimodal Floquet theoretical treatment, J. Chem. Phys. 115 (2001) 8983–9000.
[17] M. Mehring, J.S. Waugh, Magic-angle NMR experiments in solids, Phys. Rev. B5 (1972) 3459–3471.
[18] M.H. Levitt, A. Bielecki, A.C. Kolbert, D.J. Ruben, High-resolution 1H NMR in solids with frequency-switched multiple-pulse sequences, Solid State NMR 2 (1993) 151–163.

[19] D. Sakellariou, A. Lesage, P. Hodgkinson, L. Emsley, Homonuclear dipolar decoupling in solid-state NMR using continuous phase modulation, Chem. Phys. Lett. 319 (2000) 253–260.
[20] S.P. Brown, Probing proton–proton proximities in the solid state, Prog. Nucl. Magn. Reson. Spectrosc. 50 (2007) 199–251.
[21] E. Vinogradov, P.K. Madhu, S. Vega, Proton spectroscopy in solid state nuclear magnetic resonance with windowed phase modulated Lee–Goldburg decoupling sequences, Chem. Phys. Lett. 354 (2002) 193–202.
[22] A. Lesage, D. Sakellariou, S. Hedier, B. Elena, P. Charmont, S. Steuerngel, L. Emsley, Experimental aspects of proton NMR spectroscopy in solids using phase-modulated homonuclear dipolar decoupling, J. Magn. Reson. 163 (2003) 105–113.
[23] A. Samoson, T. Tuherm, J. Past, A. Reinhold, T. Anupold, I. Heinmaa, New horizons for magic-angle spinning NMR, Topics Curr. Chem. 246 (2005) 15–31.
[24] P.K. Madhu, X. Zhao, M.H. Levitt, High-resolution 1H NMR in the solid state using symmetry-based pulse sequences, Chem. Phys. Lett. 346 (2001) 142–148.
[25] S. Paul, R.S. Thakur, P.K. Madhu, 1H homonuclear dipolar decoupling at high magic-angle spinning frequencies with rotor-synchronised symmetry sequences, Chem. Phys. Lett. 456 (2008) 253–256.
[26] J.P. Amoureux, B. Hu, J. Trebosc, Enhanced resolution in proton solid-state NMR with very-fast MAS experiments, J. Magn. Reson. 193 (2008) 305–307.
[27] J.P. Amoureux, B. Hu, J. Trebosc, F. Deng, Homonuclear dipolar decoupling schemes for fast MAS, Solid State NMR 35 (2009) 19–24.
[28] M. Leskes, S. Steuernagel, D. Schneider, P.K. Madhu, S. Vega, Homonuclear dipolar decoupling at magic-angle spinning frequencies up to 65 kHz in solid-state nuclear magnetic resonance, Chem. Phys. Lett. 466 (2008) 95–99.
[29] E. Salager, R.S. Stein, S. Steuernagel, A. Lesage, B. Elena, L. Emsley, Enhanced sensitivity in high-resolution 1H solid-state NMR spectroscopy with DUMBO dipolar decoupling under ultra-fast MAS, Chem. Phys. Lett. 469 (2009) 336–341.
[30] J.H. Shirley, Solution of the Schrodinger equation with a Hamiltonian periodic in time, Phy. Rev. B138 (1965) 979–987.
[31] S. Vega, Floquet theory, in: D.M. Grant, R.K. Harris (Eds.), Encyc. of NMR, John Wiley & Sons, Chichester, 1996.
[32] A.E. Bennett, R.G. Griffin, S. Vega, Recouling of homo-heteronuclear dipolar interactions in rotating solids, NMR Basic Princ. Prog. 33 (1994) 1–77.
[33] G.J. Boender, S. Vega, H.J.M. De Groot, A physical interpretation of the Floquet description of magic angle spinning nuclear magnetic resonance spectroscopy, Mol. Phys. 95 (1998) 921–934.
[34] J.H. van Vleck, On U3c3-type doubling and electron spin in the spectra of diatomic molecules, Phys. Rev. 33 (1929) 467–506.
[35] M. Leskes, P.K. Madhu, S. Vega, A broad-banded *z*-rotation windowed phase-modulated Lee–Goldburg pulse sequence for 1H spectroscopy in solid-state NMR, Chem. Phys. Lett. 447 (2007) 370–374.
[36] M. Leskes, P.K. Madhu, S. Vega, Supercycled homonuclear dipolar decoupling in solid-state NMR: toward cleaner 1H spectrum and higher spinning rates, J. Chem. Phys. 128 (2008) 52309–52320.
[37] M. Veshtort, R.G. Griffin, SPINEVOLUTION: a powerful tool for the simulation of solid and liquid state NMR experiments, J. Magn. Reson. 178 (2006) 248–282.
[38] M. Leskes, P.K. Madhu, S. Vega, Proton line narrowing in solid-state nuclear magnetic resonance: new insights from windowed phase-modulated Lee–Goldburg sequence, J. Chem. Phys. 125 (2006) 124506–124524.
[39] L. Bosman, P.K. Madhu, S. Vega, E. Vinogradov, Improvement of homonuclear dipolar decoupling sequences in solid-state nuclear magnetic resonance utilising radiofrequency imperfections, J. Magn. Reson. 169 (2004) 39–48.